Langmuir
Article
pubs.acs.org/Langmuir

Specific Anion Effects on Water Structure Adjacent to Protein Monolayers†

Xin Chen, Sarah C. Flores, Soon-Mi Lim, Yanjie Zhang, Tinglu Yang, Jaibir Kherb, and Paul S. Cremer*

Department of Chemistry, Texas A&M University, College Station, Texas 77843

Received April 20, 2010. Revised Manuscript Received June 4, 2010

Vibrational sum frequency spectroscopy (VSFS) was used to explore specific ion effects on interfacial water structure adjacent to a bovine serum albumin (BSA) monolayer adsorbed at the air/water interface. The subphase conditions were varied by the use of six different sodium salts and four different pH values. At pH 2 and 3, the protein layer was positively charged and it was found that the most chaotropic anions caused the greatest attenuation of water structure. The order of the salts followed an inverse Hofmeister series. On the other hand, when the protein layer was near its isoelectric point (pH 5), the most chaotropic anions caused the greatest increase in water structure, although the effect was weak. In this case, a direct Hofmeister series was obeyed. Finally, virtually no effect was observed when the protein layer was negatively charged with a subphase pH of 9. For comparison, similar experiments were run with positively charged, negatively charged, and zwitterionic surfactant monolayers. These experiments gave rise to nearly the identical results as the protein monolayer which suggested that specific anion effects are dominated by the charge state of the interfacial layer rather than its detailed chemical structure. In a final set of experiments, salt effects were examined with a monolayer made from an elastin-like polypeptide (ELP). The peptide consisted of 120 pentameric repeats of the sequence Val-Pro-Gly-Val-Gly. Data from this net neutral biopolymer followed a very weak, but direct Hofmeister series. This suggested that direct anion binding to the amide groups in the backbone of a polypeptide is quite weak in agreement with the BSA data. The results from the variously charged protein, surfactant, and polymer monolayers were compared with a modified Gouy−Chapman−Stern model. The agreement with this simple model was quite good.

Introduction

Specific Ion Effects and the Hofmeister Series. The Hofmeister series represents an ordering of ions that widely influence chemical and physical processes in biological and colloidal systems.[1,2] The series was discovered in 1888 by Franz Hofmeister whereby it was shown that ions had consistent effects on the solubility of proteins.[3,4] Over the intervening 12 decades, it has been found that a wide range of physical phenomena concerning colloidal systems of oil, water, and salt obey the Hofmeister series. Particular examples include protein stability,[5,6] enzyme activity,[7−10] protein−protein interactions,[11,12] protein crystallization,[13] optical rotation of sugars and amino acids,[14] bacterial growth,[15] the surface tension of aqueous interfaces,[16,17] micelle formation,[18−20] membrane permeability,[21] and the phase behavior of monolayers and macromolecules.[22−25] The typical order for the relative effectiveness of common inorganic anions on the solubility of proteins is as follows:

$$SO_4^{2-} > F^- > Cl^- > NO_3^- > Br^- > I^- > ClO_4^- > SCN^-$$

The anions on the left side are increasingly kosmotropic. This means that they are strongly hydrated, salt proteins out of solution and prevent proteins from unfolding. Moving to the right, the anions become increasingly chaotropic. As such, they are weakly hydrated, salt proteins into solution and cause them to denature. Chloride is often considered to be the dividing line between chaotropic and kosmotropic behavior.

Traditionally, it was believed that Hofmeister ordering should be caused by changes in the hydrogen-bonding network of water

† Part of the Molecular Surface Chemistry and Its Applications special issue.

*Author to whom correspondence should be directed. E-mail: cremer@mail.chem.tamu.edu.

(1) Kunz, W.; Lo Nostro, P.; Ninham, B. W. *Curr. Opin. Colloid Interface Sci.* **2004**, *9*, 1.
(2) Zhang, Y. J.; Cremer, P. S. *Curr. Opin. Chem. Biol.* **2006**, *10*, 658.
(3) Hofmeister, F. *Arch. Exp. Pathol. Pharmakol.* **1888**, *24*, 247.
(4) Kunz, W.; Henle, J.; Ninham, B. W. *Curr. Opin. Colloid Interface Sci.* **2004**, *9*, 19.
(5) Broering, J. M.; Bommarius, A. S. *J. Phys. Chem. B* **2005**, *109*, 20612.
(6) Xiong, K.; Asciutto, E. K.; Madura, J. D.; Asher, S. A. *Biochemistry* **2009**, *48*, 10818.
(7) Pinna, M. C.; Bauduin, P.; Touraud, D.; Monduzzi, M.; Ninham, B. W.; Kunz, W. *J. Phys. Chem. B* **2005**, *109*, 16511.
(8) Pinna, M. C.; Salis, A.; Monduzzi, M.; Ninham, B. W. *J. Phys. Chem. B* **2005**, *109*, 5406.
(9) Bauduin, P.; Nohmie, F.; Touraud, D.; Neueder, R.; Kunz, W.; Ninham, B. W. *J. Mol. Liq.* **2006**, *123*, 14.
(10) Vrbka, L.; Jungwirth, P.; Bauduin, P.; Touraud, D.; Kunz, W. *J. Phys. Chem. B* **2006**, *110*, 7036.
(11) Perez-Jimenez, R.; Godoy-Ruiz, R.; Ibarra-Molero, B.; Sanchez-Ruiz, J. M. *Biophys. J.* **2004**, *86*, 2414.
(12) Curtis, R. A.; Lue, L. *Chem. Eng. Sci.* **2006**, *61*, 907.
(13) Collins, K. D. *Methods* **2004**, *34*, 300.
(14) Lo Nostro, P.; Ninham, B. W.; Milani, S.; Fratoni, L.; Baglioni, P. *Biopolymers* **2006**, *81*, 136.
(15) Lo Nostro, P.; Ninham, B. W.; Lo Nostro, A.; Pesavento, G.; Fratoni, L.; Baglioni, P. *Phys. Biol.* **2005**, *2*, 1.
(16) Ninham, B. W.; Yaminsky, V. *Langmuir* **1997**, *13*, 2097.
(17) Boström, M.; Kunz, W.; Ninham, B. W. *Langmuir* **2005**, *21*, 2619.
(18) Srinivasan, V.; Blankschtein, D. *Langmuir* **2003**, *19*, 9932.
(19) Srinivasan, V.; Blankschtein, D. *Langmuir* **2003**, *19*, 9946.
(20) Boström, M.; Williams, D. R. M.; Ninham, B. W. *Langmuir* **2002**, *18*, 6010.
(21) Hennig, A.; Fischer, L.; Guichard, G.; Matile, S. *J. Am. Chem. Soc.* **2009**, *131*, 16889.
(22) Sovago, M.; Wurpel, G. W. H.; Smits, M.; Muller, M.; Bonn, M. *J. Am. Chem. Soc.* **2007**, *129*, 11079.
(23) Aroti, A.; Leontidis, E.; Maltseva, E.; Brezesinski, G. *J. Phys. Chem. B* **2004**, *108*, 15238.
(24) Zhang, Y. J.; Furyk, S.; Bergbreiter, D. E.; Cremer, P. S. *J. Am. Chem. Soc.* **2005**, *127*, 14505.
(25) Zhang, Y. J.; Furyk, S.; Sagle, L. B.; Cho, Y.; Bergbreiter, D. E.; Cremer, P. S. *J. Phys. Chem. C* **2007**, *111*, 8916.

in bulk solution.[26] Specifically, kosmotropes were thought to be water structure makers that strengthen aqueous hydrogen-bonding, while chaotropes were believed to act as water structure breakers. However, recent experimental[24,27−31] and theoretical[32−34] investigations have cast serious doubt on this notion. In fact, it has been clearly demonstrated that bulk water structure making and breaking by salts is not central to the ion specific nature of most physical phenomena in solution. This led to the hypothesis that the Hofmeister series results from interfacial phenomena which involve the direct interaction of ions with the macromolecule/aqueous interface.[2,35]

Specific Ion Effects and Interfacial Water Structure. The interactions between salts and macromolecules are often mediated by interfacial water. It is now well established that chaotropic anions preferentially accumulate at the topmost layers of surfaces and interfaces.[29,30,33,34,36−43] Therefore, the question arises as to how interfacial water is influenced by these Hofmeister ions. The role of interfacial water structure was largely unexplored until recently, partially due to the lack of appropriate experimental tools for probing the corresponding structure. Lakshmanan et al. measured the dilatational rheology of bovine serum albumin (BSA).[44] Their results indirectly suggested that water molecules proximal to protein interfaces are affected by the presence of Hofmeister ions. Our laboratory has reported the use of vibrational sum frequency spectroscopy (VSFS) to study the effects of Hofmeister ions on interfacial water structure next to a protein-like macromolecule, poly(*N*-isopropylacrylamide) (PNIPAM).[30]

VSFS is a powerful and informative technique for studying interfacial water structure.[39,45−47] This technique relies on a nonlinear optical phenomenon called sum frequency generation (SFG). In SFG, two photons combine to produce an output photon with a frequency corresponding to the sum of the original two input frequencies (Figure 1a). In a typical VSFS experiment, an infrared beam and a visible beam are overlapped on the surface of a sample of interest as illustrated in Figure 1b. The strength of the sum frequency signal is typically enhanced when the frequency

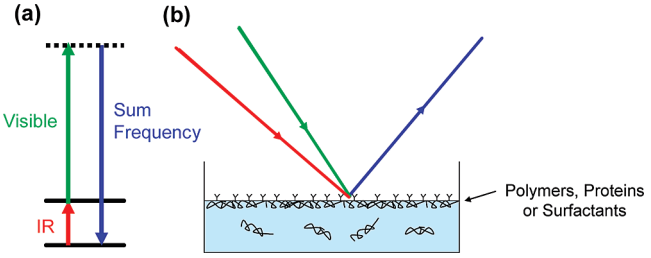

Figure 1. (a) Energy diagram for VSFS. (b) Schematic diagram of our experimental setup. The monolayer at the air/water interface represents a Gibbs monolayer of protein or polymer molecules.

of the infrared beam is on resonance with molecular vibrations from the sample. Because of its selection rules, this process is only allowed where inversion symmetry is broken. Therefore, the process is inherently surface/interface specific because surfaces naturally lack inversion symmetry.[39,45−47] At aqueous interfaces, the VSFS signal typically emanates from just a few layers of water molecules.[46]

VSFS has been applied to investigate numerous aqueous interfaces.[39,46,47] It has generally been found that the interfacial water structure is more ordered than the corresponding bulk liquid. Moreover, interfacial ordering is highly sensitive to surface hydrophobicity and the charge at the surface. Specifically, interfacial water molecules are aligned by the surface charge such that their orientation follows the direction of the local electric field. For example, interfacial water molecules preferentially orient their OH bonds toward negatively charged monolayers and away from positively charged monolayers.[48−51]

The effects of salts on interfacial water structure have been studied at air/water interfaces.[39,43,52−56] Such studies have typically focused on halide ions, which can be regarded as a subset of the Hofmeister series. Our systematic study of specific anion effects on PNIPAM were conducted with a more complete Hofmeister series.[30] These studies generally concluded that more chaotropic anions preferentially partition to the interface compared with less chaotropic anions. Moreover, metal cations are typically excluded from uncharged interfaces. Such effects are much more pronounced for the PNIPAM/water interface compared with the air/water interface.

Herein, we extend our VSFS studies of macromolecule/aqueous interfaces to a charged system, bovine serum albumin (BSA). BSA consists of primary, secondary, and tertiary protein structure which is chemically heterogeneous.[57] To understand how the charged surface influences specific ion effects, BSA/aqueous interfaces were investigated by VSFS at various pH values. It was found that the interfacial water structure can follow either a direct or inverse Hofmeister series, depending on whether the pH of the solution was below or above the isoelectric point of the protein. We also performed the same experiments on a positively

(26) Collins, K. D.; Washabaugh, M. W. *Q. Rev. Biophys.* **1985**, *18*, 323.
(27) Omta, A. W.; Kropman, M. F.; Woutersen, S.; Bakker, H. J. *Science* **2003**, *301*, 347.
(28) Batchelor, J. D.; Olteanu, A.; Tripathy, A.; Pielak, G. J. *J. Am. Chem. Soc.* **2004**, *126*, 1958.
(29) Gurau, M. C.; Lim, S. M.; Castellana, E. T.; Albertorio, F.; Kataoka, S.; Cremer, P. S. *J. Am. Chem. Soc.* **2004**, *126*, 10522.
(30) Chen, X.; Yang, T. L.; Kataoka, S.; Cremer, P. S. *J. Am. Chem. Soc.* **2007**, *129*, 12272.
(31) Smith, J. D.; Saykally, R. J.; Geissler, P. L. *J. Am. Chem. Soc.* **2007**, *129*, 13847.
(32) Boström, M.; Williams, D. R. M.; Ninham, B. W. *Phys. Rev. Lett.* **2001**, *87*, 168103.
(33) Jungwirth, P.; Tobias, D. J. *J. Phys. Chem. B* **2001**, *105*, 10468.
(34) Jungwirth, P.; Tobias, D. J. *J. Phys. Chem. B* **2002**, *106*, 6361.
(35) Jungwirth, P.; Winter, B. *Annu. Rev. Phys. Chem.* **2008**, *59*, 343.
(36) Knipping, E. M.; Lakin, M. J.; Foster, K. L.; Jungwirth, P.; Tobias, D. J.; Gerber, R. B.; Dabdub, D.; Finlayson-Pitts, B. J. *Science* **2000**, *288*, 301.
(37) Petersen, P. B.; Saykally, R. J. *Chem. Phys. Lett.* **2004**, *397*, 51.
(38) Ghosal, S.; Hemminger, J. C.; Bluhm, H.; Mun, B. S.; Hebenstreit, E. L. D.; Ketteler, G.; Ogletree, D. F.; Requejo, F. G.; Salmeron, M. *Science* **2005**, *307*, 563.
(39) Gopalakrishnan, S.; Liu, D. F.; Allen, H. C.; Kuo, M.; Shultz, M. J. *Chem. Rev.* **2006**, *106*, 1155.
(40) Pegram, L. M.; Record, M. T. *Proc. Natl. Acad. Sci. U.S.A.* **2006**, *103*, 14278.
(41) Pegram, L. M.; Record, M. T. *J. Phys. Chem. B* **2007**, *111*, 5411.
(42) Pegram, L. M.; Record, M. T. *J. Phys. Chem. B* **2008**, *112*, 9428.
(43) Liu, D. F.; Ma, G.; Levering, L. M.; Allen, H. C. *J. Phys. Chem. B* **2004**, *108*, 2252.
(44) Lakshmanan, M.; Dhathathreyan, A.; Miller, R. *Colloids Surf., A* **2008**, *324*, 194.
(45) Shen, Y. R. *The Principle of Nonlinear Optics*; John Wiley & Sons: New York, 1984.
(46) Shen, Y. R.; Ostroverkhov, V. *Chem. Rev.* **2006**, *106*, 1140.
(47) Richmond, G. L. *Chem. Rev.* **2002**, *102*, 2693.
(48) Gragson, D. E.; McCarty, B. M.; Richmond, G. L. *J. Phys. Chem.* **1996**, *100*, 14272.
(49) Gragson, D. E.; McCarty, B. M.; Richmond, G. L. *J. Am. Chem. Soc.* **1997**, *119*, 6144.
(50) Gragson, D. E.; Richmond, G. L. *J. Am. Chem. Soc.* **1998**, *120*, 366.
(51) Gragson, D. E.; Richmond, G. L. *J. Phys. Chem. B* **1998**, *102*, 3847.
(52) Shultz, M. J.; Baldelli, S.; Schnitzer, C.; Simonelli, D. *J. Phys. Chem. B* **2002**, *106*, 5313.
(53) Mucha, M.; Frigato, T.; Levering, L. M.; Allen, H. C.; Tobias, D. J.; Dang, L. X.; Jungwirth, P. *J. Phys. Chem. B* **2005**, *109*, 7617.
(54) Raymond, E. A.; Richmond, G. L. *J. Phys. Chem. B* **2004**, *108*, 5051.
(55) York, R. L.; Holinga, G. J.; Somorjai, G. A. *Langmuir* **2009**, *25*, 9369.
(56) York, R. L.; Mermut, O.; Phillips, D. C.; McCrea, K. R.; Ward, R. S.; Somorjai, G. A. *J. Phys. Chem. C* **2007**, *111*, 8866.
(57) Theodore Peters, J. *All about Albumin*; Academic Press: New York, 1996.

charged, a negatively charged, and a zwitterionic surfactant. These experiments demonstrated that the interfacial water structure near a sufficiently charged surfactant or macromolecular interface follows a general trend that depends upon its net electrostatic charge and is rather independent of the specific surface chemistry. To further aid in understanding the BSA system, we have also employed a model polypeptide, elastin-like polypeptide (ELP),[58,59] which consists of 120 pentameric repeats of VPGVG for a total of 600 residues. This simpler uncharged system is made up of nonpolar side chains and an amide backbone. Our studies reveal that the interactions of anions with backbone amides in polypeptides are rather weak in comparison to anion−amide interactions in which the amide moiety is part of the side chain.[30]

Experimental Procedures

Materials. All salts were purchased from Aldrich and used without further purification. These included Na_2SO_4, NaCl, NaBr, $NaNO_3$, $NaClO_4$, and NaSCN. It should be noted that we intentionally excluded two anions, fluoride and iodide, in these studies. Fluoride was excluded because it easily forms its complementary acid, HF, which increases the pH value of the corresponding solution. This is problematic because the charge on BSA is pH sensitive. All the anions used herein are the complementary bases of relatively strong acids and therefore only slightly perturb the pH value. We also chose not to include iodide because this anion can be easily oxidized to triiodide, I_3^-. Triiodide is a more chaotropic anion than iodide itself.[60] Since chaotropes are highly effective in altering interfacial water structure, even a small amount of triiodide could contribute significantly to the apparent response of an iodide solution. As a result, the effect of iodide could be overestimated because of such contamination.

All salt solutions were prepared by dissolving an appropriate amount of the dry material into purified H_2O produced with a NANOpure Ultrapure Water System (Barnstead, Dubuque, IA) and had a minimum resistivity of 18.1 MΩ·cm. The pH was adjusted to the desired value by the addition of either HCl or NaOH as required. The VSFS spectra obtained using freshly prepared salt solutions were indistinguishable from the results of control experiments where both the solutions and the experimental chamber were purged with N_2. We occasionally found that older solutions could produce irreproducible results.

1,2-Dipalmitoyl-3-trimethylammonium-propane (chloride salt) and 1,2-dilauroyl-*sn*-glycero-3-phosphocholine were purchased from Avanti Polar Lipids, Inc. (Alabaster, AL), and sodium 1-dodecanesulfonate came from Aldrich. The ELP was prepared by overexpression in *E. coli* following standard procedures.[58,59,61] The polypeptide was collected after cell lysis via sonication of the cells followed by several inverse phase transition temperature cycling steps for purification. Finally, the polymer was dialyzed against purified water, lyophilized, and stored at −80 °C until use.

Vibrational Sum Frequency Spectroscopy (VSFS). All experiments were performed using a standard VSFS setup as previously reported.[29,30] Briefly, a small Langmuir trough (model 601M, Nima, U.K.) with a volume of 35 mL was used to hold the salt solutions. Experiments were carried out with Gibbs monolayers of both the ELP and BSA. By contrast, the surfactants were used to form Langmuir monolayers. To perform a protein experiment, a 10 mg/mL BSA solution was prepared and a 250 μL droplet of this stock solution was added to a 35 mL salt solution already in the trough. A minimum of 10 min was allotted for complete monolayer formation before any VSFS experiments were performed. Waiting longer did not appear to change the spectra within experimental error. It was found that adding the concentrated droplet of BSA solution above the subphase gave rise to highly repeatable results, whereas premixing the BSA and salt solutions followed by introduction to the trough caused much longer waiting times for complete monolayer formation to occur. Gibbs monolayers of ELPs were prepared in a similar fashion except that a 2 mg/mL stock solution was employed and complete monolayer formation appeared to proceed even faster. For Langmuir monolayers, a droplet of surfactant solution in chloroform (~10 μL depending on the molecular weight of the surfactant) at a concentration of 1 mg/mL was introduced on top of the desired salt solution in the trough. The surface tension was then adjusted to 15 mN/m by sliding barriers. The pressure was measured with a paper Wilhelmy plate.[62]

Visible and infrared beams were synchronized and focused onto the surface of the aqueous solution. A custom-built Nd:YAG laser (Continuum, Inc.) was used as the common laser source. The fundamental 1064 nm beam had an energy of 50 mJ/pulse with a 17 ps pulse duration. The laser was run at 20 Hz. The 532 nm visible beam was produced by frequency doubling, and the infrared beam was generated with an optical parametric generator/amplifier (OPG/OPA) stage from LaserVision (Bellevue, WA). In this study, the IR frequency was set to be continuously tunable between 2800 and 3750 cm^{-1} with a typical power of ~0.6 mJ/pulse at the sample surface. The 532 nm beam was 1 mJ/pulse.

The intensity of the SFG signal, I_{SFG}, was proportional to the intensities of the incoming visible and infrared laser beams, I_{vis} and I_{IR}, respectively:

$$I_{SFG} \propto |\chi_{eff}^{(2)}|^2 I_{vis} I_{IR} \quad (1)$$

where $\chi_{eff}^{(2)}$ is the effective second order nonlinear susceptibility. VSFS spectra were obtained by scanning the infrared frequency while holding the visible frequency fixed. The sum frequency response was recorded with a photomultiplier tube (Hamamatsu, Japan). All VSFS data were acquired with the ssp (s-sum frequency, s-visible, and p-infrared) polarization combination and were subject to background subtraction and normalization against the nonresonant response from a piece of Z-cut crystalline quartz. Herein, VSFS data are reported in arbitrary units. However, the same scale was used for all spectra; therefore, the intensities can be directly compared. The normalized spectra were fit to eq 2 to abstract the oscillator strengths, A_q, of the corresponding resonances:

$$\chi_{eff}^{(2)} = \chi_{NR}^{(2)} + \chi_{R}^{(2)} = \chi_{NR}^{(2)} + \sum_q \frac{A_q}{\omega_{IR} - \omega_q + i\Gamma_q} \quad (2)$$

where $\chi_{NR}{}^{(2)}$ and $\chi_{R}{}^{(2)}$ are the nonresonant and the resonant terms, respectively. For $\chi_{R}{}^{(2)}$, the qth resonant mode is a function of the oscillation strength, A_q, the resonant frequency, ω_q, the peak width, Γ_q, and the frequency of the infrared laser beam, ω_{IR}.

Results

BSA. Figure 2 shows VSFS spectra of BSA monolayers under various pH and salt conditions. The frequency range for all spectra can be divided into two regions: CH vibrations (typically 2800−3100 cm^{-1}) and OH vibrations (> 3100 cm^{-1}). Regardless of the pH or salt conditions, several sharp features could be observed in the CH stretch region. Among them, a major peak at 2880 cm^{-1} can be assigned to the methyl symmetric stretch from hydrophobic

(58) Meyer, D. E.; Chilkoti, A. *Biomacromolecules* **2004**, *5*, 846.
(59) Meyer, D. E.; Chilkoti, A. *Biomacromolecules* **2002**, *3*, 357.
(60) Cacace, M. G.; Landau, E. M.; Ramsden, J. J. *Q. Rev. Biophys.* **1997**, *30*, 241.
(61) Cho, Y. H.; Zhang, Y. J.; Christensen, T.; Sagle, L. B.; Chilkoti, A.; Cremer, P. S. *J. Phys. Chem. B* **2008**, *112*, 13765.
(62) Adamson, A. W.; Gast, A. P. *Physical Chemistry of Surfaces*; Wiley: New York, 1997.

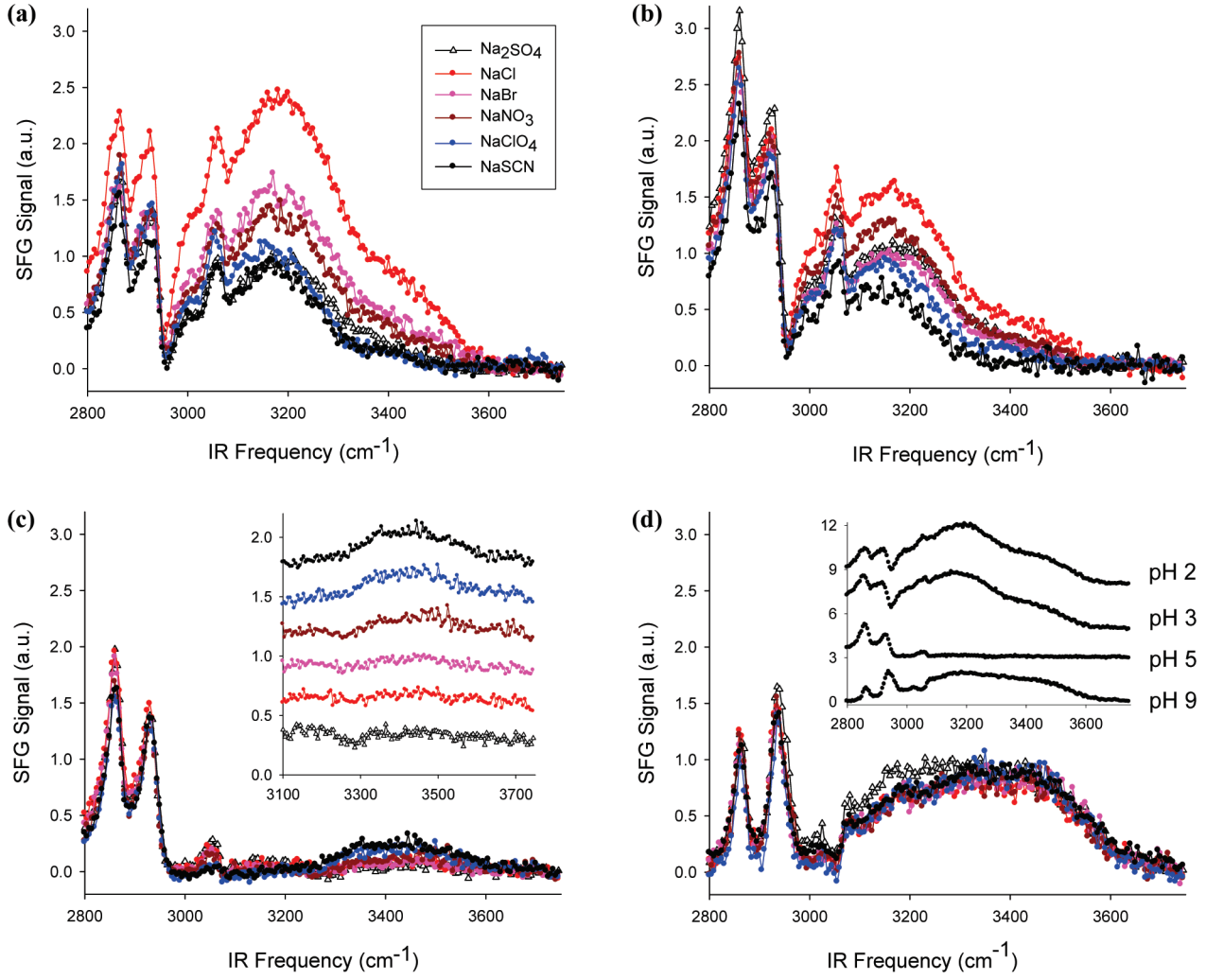

Figure 2. VSFS spectra of BSA monolayers under various pH conditions: (a) pH 2, (b) pH 3, (c) pH 5, and (d) pH 9. The inset in (c) shows a blowup of the OH stretch region. The inset in (d) shows control experiments for BSA monolayers without additional salt under the various pH conditions. All experiments in the main panels were performed with 100 mM of each salt except for sodium sulfate, which was used at 33 mM to maintain constant ionic strength. The color coded key for each ion is shown as an inset in (a).

residues on the protein.[63−65] The weak shoulder near 2840 cm^{-1} arises from the CH_2 symmetric stretch. The other major peak around 2950 cm^{-1} is a combination of a Fermi resonance and the methyl asymmetric stretch. A small peak at ~2915 cm^{-1}, which is sandwiched between the two major peaks, can occasionally be distinguished. This resonance is attributed to the methine stretch, especially from isopropyl groups in valine or isoleucine. Another small peak can be found near 3050 cm^{-1}. This feature is due to an aromatic CH stretch from residues such as phenylalanine. The substantial strength of the features in the CH stretch region is a manifestation of the partial reordering of hydrophobic moieties within the protein layer to face up into the air. These frequencies remain unaltered as the solution conditions are varied as has been previously shown by control experiments with D_2O.[63−65]

The OH stretch region contains two major peaks centered near 3200 and 3450 cm^{-1}, respectively. Their broadness has been interpreted to be due to the highly heterogeneous nature of the H-bonded structure.[39,46,47] These two peaks have been observed in VSFS measurements of virtually all charged aqueous interfaces.[39,46,47] They are often loosely referred to as "icelike" and "liquidlike" interfacial water structures.[46] These designations come from analogies with Fourier transform infrared data where ice shows an absorption centered near 3200 cm^{-1}, while liquid water has a broader peak near 3450 cm^{-1} with a modest shoulder at ~3200 cm^{-1}. It is often believed that the two VSFS features arise from water molecules with more complete and less complete hydrogen bonding networks, respectively,[46] although this notion is still a matter of some debate.[66,67]

The oscillator strengths of the OH peaks, unlike those of the CH stretches, depend greatly on the pH value of the subphase. It is well established that the intensity of these peaks is related to surface charge density.[39,46,47] Generally speaking, the higher the charge density, the more prominent these features are. BSA contains roughly 100 positively and 100 negatively chargeable residues.[57] The isoelectric point of this biomacromolecule lies near pH 5. Like all proteins, the net charge on BSA depends upon the solution pH. Under the conditions of these experiments, the monolayer should be positively charged at pH 2 (Figure 2a) and pH 3 (Figure 2b), but close to its isoelectric point at pH 5

(63) Wang, J.; Buck, S. M.; Chen, Z. *J. Phys. Chem. B* **2002**, *106*, 11666.
(64) Chen, X.; Sagle, L. B.; Cremer, P. S. *J. Am. Chem. Soc.* **2007**, *129*, 15104.
(65) Kim, G.; Gurau, M.; Kim, J.; Cremer, P. S. *Langmuir* **2002**, *18*, 2807.
(66) Sovago, M.; Campen, R. K.; Wurpel, G. W. H.; Müller, M.; Bakker, H. J.; Bonn, M. *Phys. Rev. Lett.* **2008**, 100.
(67) Nihonyanagi, S.; Yamaguchi, S.; Tahara, T. *J. Am. Chem. Soc.* **2010**, *132*, 6867.

(Figure 2c). The net charge becomes negative near pH 9 (Figure 2d). In fact, according to pH titration experiments, the net charge on BSA molecules in bulk aqueous solution should be +95, +70, 0, and −25, respectively, under these conditions.[57,68] The protein molecules may be slightly differently charged at air/water under these conditions.[69] Nevertheless, the trend of becoming more negatively charged as the pH increases should remain the same. Moreover, it would appear from Figure 2c that the isoelectric point remains close to pH 5, as this is the value at which the OH stretch features reach a minimum.

Figure 2 shows the specific ion effects under all four pH conditions in the presence of 100 mM NaSCN, 100 mM $NaClO_4$, 100 mM $NaNO_3$, 100 mM NaBr, 100 mM NaCl, and 33 mM Na_2SO_4 in the subphase. The concentration of Na_2SO_4 was chosen to match the ionic strength of the other five solutions. The specific ion effects are particularly pronounced at pH 2. Moreover, chaotropic anions, such as perchlorate and thiocyanate, give rise to spectra with the smallest water peaks. By contrast, these features are much more prominent when the chloride ion is present. The trend follows an inverse Hofmeister series as is typical for positively charged proteins. For example, lysozyme displays an inverse Hofmeister series as it is more soluble in solutions with kosmotropes than chaotropes.[70−74] Significantly, the inverse series seen in Figure 2a is only valid for monovalent anions as sulfate behaves much like the chaotropes. Such behavior with divalent anions is also seen in the solubility of lysozyme.

The spectra at pH 3 (Figure 2b) are very similar to those at pH 2, except that the water peaks are correspondingly weaker. This is consistent with the weaker net positive charge. Importantly, the ordering of the monovalent anions remains the same. On the other hand, sulfate gives rise to water peaks with roughly the same intensity as bromide rather than perchlorate as seen in Figure 2a. The intensity of the OH peaks continues to diminish as the pH is increased to the isoelectric point (Figure 2c). The inset shows blowups of the OH stretch region for ease of visualization. Strikingly, the ordering of the spectra have now inverted to a direct Hofmeister series with thiocyanate and perchlorate giving rise to the greatest amount of water structure. The smallest OH stretch peaks for this case arise from chloride and sulfate. Indeed, the divalent anion reverts to its regular position in a direct Hofmeister series. Finally, the data from the spectra at pH 9 show almost no evidence for a specific anion effect (Figure 2d). With the exception of sulfate, all spectra essentially display identical OH stretch intensity within the noise limits of the experiments. These results are consistent with the notion that the negatively charged surface repels the anions, which in turn allows for little differentiation. On the other hand, the anions should be most concentrated near the interface when the surface bears the highest positive charge, hence giving rise to the most prominent specific ion effects.

As noted above, sulfate appears in its usual position in the direct Hofmeister series (Figure 2c), but it migrates in position when the protein surface is positively charged (Figure 2a,b).[75] In other words, its apparent behavior is more like a chaotropic anion when the protein bears a positive charge. In fact, its apparent behavior becomes ever more chaotropic as the positive charge density at the interface is increased. This phenomenon can be explained on the basis of electrostatic interactions. Because sulfate is a doubly charged anion, it is subject to much stronger charge−charge interactions than singly charged anions. Once adsorbed at the interface, it is doubly effective at neutralizing the net positive charge. Moreover, its site of interaction at the protein surface is probably different from that of its monovalent counterparts. Specifically, the monovalent chaotropes may directly interact with the protons from the NH moieties on the prevalent amide moieties in the protein backbone.[76] Sulfate, on the other hand, will not shed its hydration shell to interact with these amide groups.[24] More likely, the divalent anion interacts with charged lysine and arginine residues on the protein surface.

Charged Surfactants. In order to better understand the origins of the direct and inverse Hofmeister series for the monovalent anions, we undertook studies with three different surfactant monolayers: 1,2-dipalmitoyl-3-trimethylammonium-propane (chloride salt) (DPTAP), 1,2-dilauroyl-*sn*-glycero-3-phosphocholine (DLPC), and sodium 1-dodecanesulfonate (DS). DPTAP is a positively charged double chain surfactant, DLPC is a net neutral (zwitterionic) lipid, and DS is a negatively charged single chain surfactant. It should be noted that none of the charges on these three molecules are titratable under the conditions of these experiments. All experiments were carried out without any buffer, and control experiments were performed to confirm that varying the pH did not significantly affect the spectra (data not shown). VSFS spectra for the three surfactant monolayers are provided in Figure 3a−c in the presence of the six sodium salt solutions. Data for the same three monolayers in the absence of salt are provided in Figure 3d for comparisons.

All spectra contain two groups of peaks at 2880 and 2950 cm^{-1} in the CH region. The 2880 cm^{-1} feature arises from the methyl symmetric stretch, while the shoulder on the red side of the peak comes from the methylene symmetric stretch. The 2950 cm^{-1} peaks consist of intensity from both a Fermi resonance and the methyl asymmetric stretch. In the OH stretch region in the absence of salt, there is relatively strong water intensity for the negatively and positively charged surfactants, but much more moderate intensity when neutral lipids are employed, as expected (Figure 3d). On the other hand, in the presence of the six salts, there is an inverted Hofmeister series associated with the positively charged monolayer, a direct Hofmeister series for the neutral monolayer, and essentially no specific anion effects when the monolayer is negatively charged. This is strikingly similar to the behavior of the water peaks for the BSA monolayers below, at, and above the isoelectric point, respectively. These observations are consistent with the notion that net surface charge, rather than the detailed chemical structure of the protein or surfactant interface, is the dominant factor governing specific ion effects on the alignment of interfacial water molecules for these types of systems. Interestingly, recent simulations suggest that changing surface polarity from hydrophilic to hydrophobic may also lead to Hofmeister series reversal.[77] All the systems investigated herein, however, would be deemed relatively hydrophobic as would most protein/water, lipid membrane/water, and biopolymer/water interfaces.

A Neutral Polypeptide. In the final set of experiments, we wished to take VSFS data from a neutral polypeptide. We

(68) Tanford, C.; Swanson, S. A.; Shore, W. S. *J. Am. Chem. Soc.* **1955**, *77*, 6414.
(69) Lu, J. R.; Su, T. J.; Penfold, J. *Langmuir* **1999**, *15*, 6975.
(70) Rieskautt, M. M.; Ducruix, A. F. *J. Biol. Chem.* **1989**, *264*, 745.
(71) Rieskautt, M. M.; Ducruix, A. F. *J. Cryst. Growth* **1991**, *110*, 20.
(72) RiesKautt, M.; Ducruix, A. *Methods Enzymol.* **1997**, *276*, 23.
(73) Zhang, Y. J.; Cremer, P. S. *Proc. Natl. Acad. Sci. U.S.A.* **2009**, *106*, 15249.
(74) Boström, M.; Tavares, F. W.; Finet, S.; Skouri-Panet, F.; Tardieu, A.; Ninham, B. W. *Biophys. Chem.* **2005**, *117*, 217.
(75) The sodium sulfate solution also behaves slightly differently from other ions at pH 9, which can be attributed to sodium. To keep the ionic strength the same, the concentration of sodium in the sodium sulfate solution is only two-thirds that of others. As we will discuss later, cation adsorption can be enhanced by strong negative charges, such as in this case.
(76) Tadeo, X.; Pons, M.; Millet, O. *Biochemistry* **2007**, *46*, 917.
(77) Schwierz, N.; Horinek, D.; Netz, R. R. *Langmuir* **2010**, *26*, 7370.

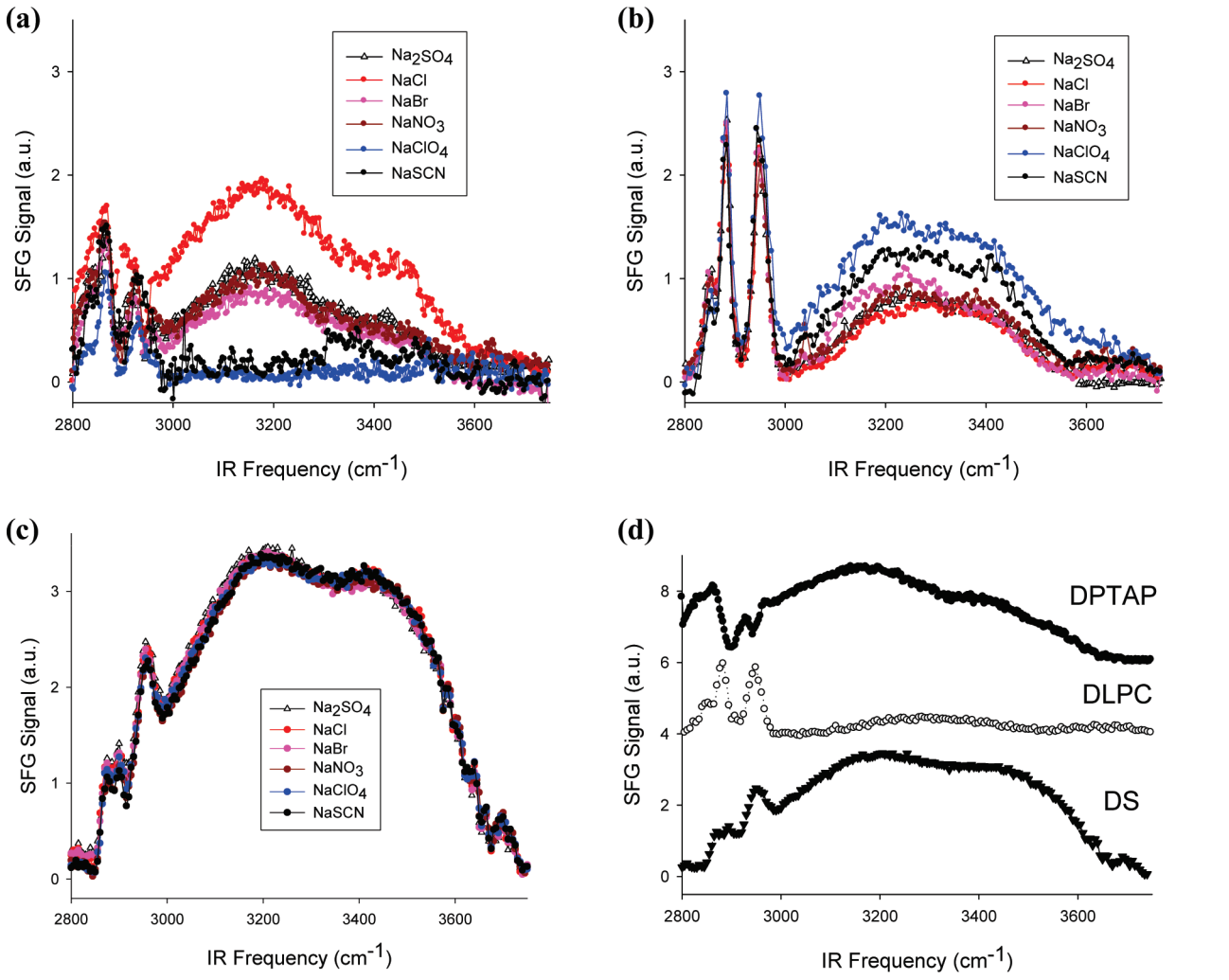

Figure 3. VSFS spectra for six sodium salts in the presence of (a) a DPTAP monolayer (positively charged), (b) a DLPC monolayer (net neutral), and (c) a DS monolayer (negatively charged). (d) Control experiments with the same three surfactants in the absence of salt. In this case, the data are offset for clarity.

therefore chose to use a Gibbs monolayer of an elastin-like polypeptide (0.005 mg/mL) with the molecular formula $(Val\text{-}Pro\text{-}Gly\text{-}Val\text{-}Gly)_{120}$ (Figure 4). The motivation for these experiments came from the fact that the OH stretch range features in Figure 2c were quite small. Moreover, the ion specific effects were also rather modest as well. Such results stand in stark contrast to our previous data with poly(*N*-isopropylacrylamide) (PNIPAM) monolayers, where strong water peaks were observed.[30] The putative binding sites for the chaotropic Hofmeister anions are the NH moieties on the amide groups.[76] Like a protein, the neutral PNIPAM polymer contains amides, but these groups are part of the side chain rather than the backbone in that case. Another example of relatively strong water peaks in the presence of salts at a neutral interface comes from Figure 3b, where the lipid layer clearly shows greater OH intensity compared with Figure 2c. Therefore, we wondered if a weak direct Hofmeister series was a general phenomenon for neutral polypeptides.

In Figure 4, there are four peaks from the ELP monolayer in the CH stretch range. These can be assigned as follows: 2880 cm^{-1} (methyl symmetric stretch), 2915 cm^{-1} (methine stretch), 2940 cm^{-1} (Fermi resonance), and 2980 cm^{-1} (methyl asymmetric stretch). In the OH stretch region, the resonances near ~3200 and ~3450 cm^{-1} are markedly weak even in the presence of the most chaotropic anions. The oscillator strengths in the OH stretch

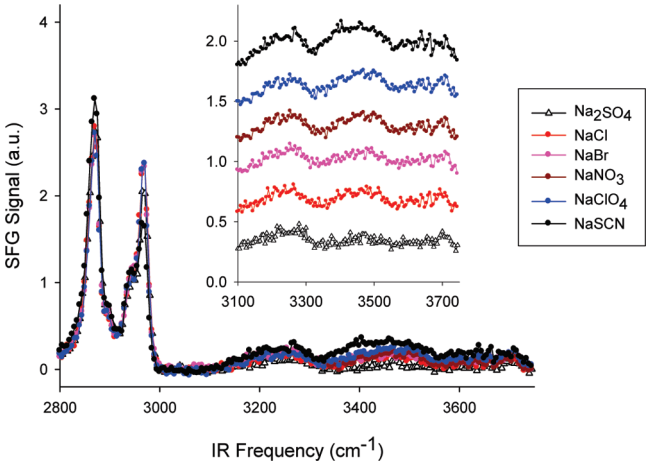

Figure 4. Specific anion effects on ELPs adsorbed at the air/water interface. To avoid crowding, the same data in the OH region are provided as an inset where they are offset and magnified.

region are approximately 1 order of magnitude weaker for the ELP than for the neutral lipid layer shown in Figure 3b or for PNIPAM. They are, however, quite similar to the features seen in Figure 2c for the neutral BSA layers. Again, a direct Hofmeister

series is followed with the most chaotropic anions leading to the most significant (albeit modest) OH stretch intensity. Such a result is consistent with the notion that when amide moieties are part of the polymer backbone, they are relatively inaccessible to direct interactions with chaotropic anions compared with the case where these same functional moieties are part of the side chain. Indeed, the interfacial water structure changes induced by ions on the ELP are similar to those found at the bare air/water interface, where no additional functional groups exist.[39,43,52−54] In both systems, the water peaks are only slightly enhanced even with the addition of the most chaotropic anions. Finally, it should be noted that the results in Figures 2c and 4 are consistent with previous inverse phase transition measurements of PNIPAM and ELP in bulk aqueous solutions, which also found that the anions bound more strongly to PNIPAM than to neutral ELPs.[24,61]

Discussion

Interfacial water structure at charged and neutral macromolecular interfaces appears to share some very generic anion dependent characteristics. Specifically, it appears that the water structure only marginally varies with the nature of the surface chemistry. Rather, the net charge at the interface appears to be the dominant factor in determining a system's interfacial water structure and salt behavior. This idea can be summarized as follows: neutral surfaces generally display relatively modest specific anion effects and follow a direct Hofmeister series. Positively charged surfaces induce greater specific anion effects with an inverse Hofmeister series. Moreover, the greater the positive surface charge, the stronger these effects appear to be. On the other hand, if the surface is highly negatively charged, there are virtually no specific anion effects. As will be discussed below, these phenomena can be understood in terms of the preferential adsorption of more chaotropic monovalent anions, over less chaotropic monovalent anions. As such, even the addition of 10 mM Cl^-, which was used to create the pH 2.0 solutions in Figure 2a, should have had only a minimal effect on the water structures observed.

Ion Adsorption and Gouy−Chapman−Stern Theory. When ions adsorb to an interface, the surface potential is altered. From earlier VSFS studies, it is known that water peaks are mostly generated via the local electric fields which align interfacial water molecules.[39,46,47] In fact, linear correlations under certain conditions have been reported between the oscillator strengths of the water peaks and the surface potential.[30,48−51] The fact that the VSFS signal is proportional to the square of the surface potential makes it a sensitive tool for monitoring changes in the interfacial water structure and therefore net anion absorption.

Ion adsorption can be physically viewed as the equilibrium of ion partitioning between the bulk solution and the interfacial layer. The number density of adsorbed ions can therefore be regarded as the surface concentration of these ions. If there is an overall attractive interaction between the ion and the surface, then the ion will accumulate at the surface until it is balanced by the electrochemical potential. This equilibrium partitioning depends on the intrinsic binding strength, the bulk ion concentration, and the charge density at the surface. As shown previously, the effects of ion adsorption on surface potential can be modeled with a modified version of Gouy−Chapman−Stern theory for initially uncharged systems.[30] Below, we will extend this model to apply to systems which initially bear a net negative or positive charge.

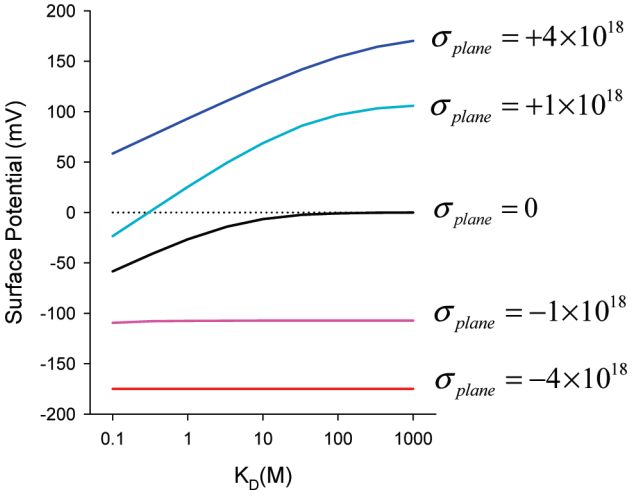

Figure 5. The calculated surface potential for anion adsorption at various σ_{plane} values (unit: m^{-2}) as a function of the equilibrium dissociation constant, K_D. The salt concentration is set at 100 mM and the density of the binding sites is set at 5×10^{18} m^{-2}. Both the anions and cations are assumed to be monovalent. Moreover, the interaction of the surface with the cations is assumed to be negligible. Note that the bottom (red) and top (blue) curves represent nearly limiting cases of very high negative charge density and very high positive charge density, respectively.

According to the Stern model, the adsorption of an ion can be described by a Langmuir model with an extra electrostatic term.[62]

$$\sigma_{adsorption} = \frac{zeN_s\frac{C}{K_D}\exp\frac{ze\varphi(0)}{kT}}{1+\frac{C}{K_D}\exp\frac{ze\varphi(0)}{kT}} \quad (3)$$

where $\sigma_{adsorption}$ is the surface density of adsorbed ions, z is the valence of the ions, C is the bulk ion concentration, K_D is the equilibrium dissociation constant, and N_s is the number density of binding sites. The exponential term in the equation is simply an electrochemical potential in which $\varphi(0)$ is the surface potential and kT is the thermal energy. Note that this equation is not directly useful, since both $\sigma_{adsorption}$ and $\varphi(0)$ are unknown.

A charged plane contacting an electrolyte solution induces a diffuse double layer that carries a net charge of opposite sign. The overall charge density in this double layer is dictated by Gouy−Chapman theory:[62]

$$\sigma_{diffuse} = -(8I\varepsilon_r\varepsilon_0kT)^{1/2}\sinh\frac{ze\varphi(0)}{2kT} \quad (4)$$

where $\sigma_{diffuse}$ is the net charge density, I is the ionic strength, ε_r is the dielectric constant, and ε_0 is the permittivity of vacuum. Other parameters and variables are the same as those in eq 3.

Finally, eq 5 has to be obeyed to guarantee electric neutrality:

$$\sigma_{diffuse} + \sigma_{adsorption} + \sigma_{plane} = 0 \quad (5)$$

where σ_{plane} is the surface charge density in the absence of ion adsorption. With three unknowns, $\sigma_{adsorption}$, $\sigma_{diffuse}$, and $\varphi(0)$, and three equations, the problem can be solved. The solution for this set of equations is very sensitive to σ_{plane} as well as K_D. The system will behave rather differently under different conditions. In the following, we will outline a couple of representative cases and compare them with the experimental results provided above.

σ_{plane}, K_D, and Specific Ion Effects. The specific anion effects on the oscillator strength of the water peaks can be modeled as a surface potential dependence on K_D, the only ion specific term in the equations. Examples of the variation of K_D with surface potential are shown in Figure 5. The black curve in this figure represents the situation for an initially uncharged system, $\sigma_{plane} = 0$. Not surprisingly, the surface potential dependence on K_D is monotonic and anions that bind more tightly (smaller K_D) yield a more negative surface potential. The slope of this curve represents the sensitivity of the surface potential to K_D, which in turn is related to the magnitude of the specific ion effect on interfacial water alignment. From the curve, one can see that the slope actually depends on the absolute value of K_D; it is virtually flat when the binding is weak ($K_D > 10$ M), but it becomes steeper with increasing binding strength. This result is consistent with our experimental observation that only more chaotropic anions bind to the interface, rather than species such as Cl^-.

We have previously shown that the apparent dissociation constants for anions with the pendent amide moieties of PNIPAM are in the range of 0.15−15 M.[30] Therefore, one might expect similar results for neutral polypeptides. However, anion adsorption to BSA at pH 5 or to the ELP (both net neutral polymers) was found to be very weak and to display only very weak anion specificity. Therefore, based upon the model provided in Figure 5 (black curve), the equilibrium dissociation constant for even the most chaotropic anion (e.g., thiocyanate) should be ≥20 M. This result almost certainly stems from the relative inaccessibility of amide moieties present in the backbone of polypeptides versus the more available pendent amide moieties found on PNIPAM. Finally, it should be noted that cations in general and Na^+ in particular do not adsorb to neutral macromolecules containing amide moieties nearly as well as chaotropic anions do.[30] This is not surprising because they are usually smaller, less polarizable, and better solvated than the anions.[78] As such, the surface potential is little affected by them.

Charged surfaces behave very differently from neutral ones. Indeed, specific ion effects depend greatly on the sign as well as the magnitude of σ_{plane}. In addition to the initially neutral case, Figure 5 also shows how the surface potential changes with K_D for two positive and two negative σ_{plane} values. The steepness of these curves roughly indicates the magnitude of ion specific effects on surfaces with different initial charges. As can be seen, the curve is clearly steeper when the charge on the surface is more positive. Even moderately weak binding anions can be distinguished from very weak binders. By contrast, when the surface bears a negative charge, the curves are nearly flat even as K_D approaches 100 mM. These situations can be illustrated in the following example. Let us compare an anion with $K_D = 1$ M to another anion that binds 100 times more weakly ($K_D = 100$ M). It should be noted that the latter anion essentially does not bind specifically to the surface under physically relevant conditions. On a neutral surface, these two ions will generate a potential of −26.7 and −0.8 mV, respectively, as shown by the black curve in Figure 5. On the other hand, if the surface bears a positive charge ($\sigma_{plane} = 1 \times 10^{18}$ m^{-2}, the cyan curve), the surface potential induced by the same two ions will be +25.4 and +96.9 mV, respectively. This represents a much greater absolute difference (71.5 mV vs 25.9 mV) with reversed order. Finally, if the surface carries the same amount of charge with a negative sign ($\sigma_{plane} = -1 \times 10^{18}$ m^{-2}, the pink curve), the ultimate surface potentials will be −107.5 and −107.3 mV, respectively. This difference is far too small to be measured experimentally. This model matches extremely well with the experimental observations on the variously charged surfaces of BSA (Figure 2) as well as for the surfactants (Figure 3).

Finally, it should be noted that the adsorption of anions may perturb the titration state of the originally charged surfaces, which could in turn contribute to the overall specific ion effects. In the case of BSA, anion adsorption should help protonate charged residues.[79] Such titration will help negate the effect of anion adsorption on the surface potential, thereby making specific ion effects appear to be weaker. In general, σ_{plane} will not be a constant as is assumed in the simple model above. Rather, it is a function of the protonation state of titratable residues, which can be modulated by the adsorption of anions, depending upon the pH. This effect is difficult to quantify, but it is probably only modest in the BSA system described above.

Beyond Simple Inorganic Anions. Ion adsorption to monolayer interfaces in aqueous solutions is largely dictated by a few basic physical properties, such as ion size, polarizability, and solvation energy. Therefore, most of the analysis made above may in principle be extended beyond simple inorganic ions. VSFS should be useful in studying such cases as long as the same physical principles apply. Some examples can already be found in literature. For instance, we have reported the adsorption of polydiallyldimethylammonium chloride (PDDA) on quartz surfaces.[80] PDDA, a positively charged polyelectrolyte, can be regarded as a very large and multivalent cation. One would expect that such a cation would quench the water peaks on negatively charged surfaces (e.g., fused silica) by an analogous ion adsorption mechanism with a notable specific ion effect. In fact, this is what has been observed experimentally.[80] Similarly, DNA can be regarded as a negatively charged polyelectrolyte. Therefore, DNA should adsorb to positively charged surfaces and induce changes in the interfacial water structure in a similar way, as it has also been reported in literature.[81] In these cases, one needs to consider the effects of multivalency on apparent K_D values.

Acknowledgment. We thank the National Science Foundation (CHE-0094332) and the Robert A. Welch Foundation (Grant A-1421) for funding. We also wish to thank Prof. Ashutosh Chilkoti for supplying the DNA plasmids from which the ELPs were made.

(78) Marcus, Y. *Ion Properties*; Marcel Dekker, Inc.: New York, 1997.

(79) Boström, M.; Lonetti, B.; Fratini, E.; Baglioni, P.; Ninham, B. W. *J. Phys. Chem. B* **2006**, *110*, 7563.

(80) Kim, J.; Kim, G.; Cremer, P. S. *J. Am. Chem. Soc.* **2002**, *124*, 8751.

(81) Wurpel, G. W. H.; Sovago, M.; Bonn, M. *J. Am. Chem. Soc.* **2007**, *129*, 8420.